

8. SITE 675¹

Shipboard Scientific Party²

HOLE 675A

Date occupied: 1930, 3 August 1986
Date departed: 2145, 6 August 1986
Time on hole: 3 days, 2 hr, 15 min
Position: 15°31.77'N, 58°43.01'W
Water depth (sea level, corrected m; echo-sounding): 4993.8
Water depth (rig floor, corrected m; echo-sounding): 5004.3
Bottom felt (rig floor, m; drill pipe measurement): 5018.3
Distance between rig floor and sea level (m): 10.5
Total depth (rig floor, m): 5397.2
Penetration (m): 388.1
Number of cores (including cores with no recovery): 8
Total length of cored section (m): 66.7
Total core recovered (m): 44.7
Core recovery (%): 67
Oldest sediment cored:
 Depth sub-bottom (m): 388.1
 Nature: claystone
 Age: early Miocene
 Measured velocity (km/s): 1.68

SITE 675 SUMMARY

Site 675 is located approximately 400 m west of DSDP Site 542, about 2 km west of the Barbados Ridge complex deformation front. Hole 675A penetrated 388 mbsf, taking a core at the mudline and coring the final 67 m in preparation for a packer test. The mudline core consists of lower Pleistocene foraminifera-nannofossil ooze (Unit 1). From 321 to 363 m sub-bottom we encountered barren mudstone and claystone (Unit 2), below which we penetrated 25 m of locally siliceous lower Miocene mudstone (Unit 3). Orange brown portions of Unit 3, with black manganese concentrations (especially Section 110-675A-8X-1), lithologically resemble the top of the décollement zone at Site 671. The lower Miocene radiolarian zones (R-10 through R-12) in Cores 110-675A-7X and -8X also correlate well with the top of the décollement zone at Site 671.

Prominent zones of scaly fabric occur at about 335 mbsf and 360–378 mbsf and apparently correlate with the frontal thrust and the top of the décollement zone, respectively. Relatively low chloride and high methane concentrations within or adjacent to both of these deformation zones suggest they are loci of active fluid transport. Rhodochrosite occurs in shear veins lying in, and dilatant veins cutting across, the scaly fabric of the lower deformation zone. Mineral precipitation must have occurred in the presence of near lithostatic fluid pressures necessary to hold the fractures open.

Similar to the patterns in stratigraphically equivalent rocks at Sites 671 and 672, porosity shows a localized high just above the inferred décollement. Sediments at Site 675 have an estimated *in-situ* velocity of 1.61 km/s, consistent with their high overall porosity. The low consolidation state and the active dewatering of the sediments at Site 675 produced hole-stability problems preventing any packer test.

BACKGROUND AND OBJECTIVES

Oceanic sediment entering the subduction zone in the Leg 110 area has an average porosity of about 60% (see Site 672 chapter, this volume). Reduction in porosity occurs arcward within and beneath the accretionary prism as documented by physical property data from Sites 671, 673, and 674. More substantial decreases in porosities occur during the continuing uplift and subaerial exposure of accreted sedimentary rocks (Bray and Karig, 1985). For example, the offscraped rocks exposed on the island of Barbados have a porosity of about 17%, even though they have only been buried shallowly (Larue et al., 1985). Clearly, large volumes of water must be expelled during the uplift and structural evolution of accretionary prisms. Mud volcanoes, especially common across the southern portion of the Barbados Ridge complex, are indicative of gravitational instability at depth and active dewatering (Stride et al., 1982; Westbrook and Smith, 1983; Mascle et al., 1986).

One of the principal objectives of Leg 110 was to investigate the hydrogeological evolution of the Barbados Ridge complex. The pore-water chemistry from Sites 671–674, considered in the context of the structural geology and temperature data, has provided insights on the depths of origin and flow paths of the fluids. However, understanding of the rate of fluid movement re-

¹ Mascle, A., Moore, J. C., et al., 1988. *Proc., Init. Repts. (Pt. A), ODP*, 110: College Station, TX (Ocean Drilling Program).

² J. Casey Moore (Co-Chief Scientist), Dept. of Earth Sciences, University of California at Santa Cruz, Santa Cruz, CA 95064; Alain Mascle (Co-Chief Scientist), Institut Français du Pétrole, 1–4 Ave Bois-Preau, B.P. 311, 92506 Rueil Malmaison Cedex, France; Elliott Taylor (Staff Scientist), Ocean Drilling Program, Texas A&M University, College Station, TX 77840; Francis Alvarez, Borehole Research Group, Lamont-Doherty Geological Observatory, Columbia University, Palisades, NY 10964; Patrick Andreieff, BRGM, BP 6009, 45060 Orleans Cedex-2, France; Ross Barnes, Rosario Geoscience Associates, 104 Harbor Lane, Anacortes, WA 98221; Christian Beck, Département des Sciences de la Terre, Université de Lille, 59655 Villeneuve d'Ascq Cedex, France; Jan Behrmann, Institut für Geowissenschaften und Lithosphärenforschung, Universität Giessen, Senckenbergstr. 3, D6300 Giessen, FRG; Gerard Blanc, Laboratoire de Géochimie et Métallogénie U. A. CNRS 196 U.P.M.C., 4 Place Jussieu, 75252 Paris Cedex 05, France; Kevin Brown, Dept. of Geological Sciences, Durham University, South Road, Durham, DH1 3LE, U.K. (current address: Dept. of Earth Sciences, University of California at Santa Cruz, Santa Cruz, CA 95064); Murlene Clark, Dept. of Geology, LSCB 341, University of South Alabama, Mobile, AL 36688; James Dolan, Earth Sciences Board, University of California at Santa Cruz, Santa Cruz, CA 95064; Andrew Fisher, Division of Marine Geology and Geophysics, University of Miami, 4600 Rickenbacker Causeway, Miami, FL 33149; Joris Gieskes, Ocean Research Division A-015, Scripps Institution of Oceanography, La Jolla, CA 92093; Mark Hounslow, Dept. of Geology, Sheffield University, Brook Hill, Sheffield, England S3 7HF; Patrick McLellan, Petro-Canada Resources, PO Box 2844, Calgary, Alberta Canada (current address: Applied Geotechnology Associates, 1-817 3rd Ave. NW, Calgary, Alberta T2N 0J5 Canada); Kate Moran, Atlantic Geoscience Centre, Bedford Institute of Oceanography, Box 1006, Dartmouth, Nova Scotia B2Y 4A2 Canada; Yujiro Ogawa, Dept. of Geology, Faculty of Science, Kyushu University 33, Hakozaki, Fukuoka 812, Japan; Toyosaburo Sakai, Dept. of Geology, Faculty of General Education, Utsunomiya University, 350 Mine-machi, Utsunomiya 321, Japan; Jane Schoonmaker, Hawaii Institute of Geophysics, 2525 Correa Road, Honolulu, HI 96822; Peter J. Vrolijk, Earth Science Board, University of California at Santa Cruz, Santa Cruz, CA 95064; Roy Wilkens, Earth Resources Laboratory, E34-404 Massachusetts Institute of Technology, Cambridge, MA 02139; Colin Williams, Borehole Research Group, Lamont-Doherty Geological Observatory, Columbia University, Palisades, NY 10964.

quires quantitative measurements of fluid pressures and permeabilities along the conduits. In a drilled hole such measurements are accomplished by inserting various types of probes into the sediment or by isolating a segment of the drill hole with a packer. Permeability measurements can be made on core samples and generally provide an indication of how fluid would move through the intergranular pore spaces. The few available measurements from the DSDP Leg 78A cores indicate a low permeability (about 10^{-9} cm/s at 129 mbsf; Marlow et al., 1984) as would be expected in fine-grained sediments. As the deforming sediments are more deeply buried and the intergranular permeability decreases further, it is doubtful that dewatering could occur except through a much higher fracture permeability. In fact, calcite veins in deformed mudstones at Sites 673 and 674 indicate fluid flow through fractures. Owing to its irregular distribution, reliable measurements of fracture permeability generally must be conducted *in situ*, hence the importance of the packer measurements at Site 675.

Site 675 was located just west of Site 542 at which apparently high fluid pressures were encountered during DSDP Leg 78A (Figs. 1 and 2) (Biju-Duval, Moore et al., 1984a, b). High pressures were recorded immediately after a section of drill-in casing became stuck in the hole, failed to release, and hence provided a closed conduit to the surface. The near-lithostatic pressures could have been generated by flow back of drilling-induced fluids; therefore, a true packer test is necessary to define the pressure conditions in the accretionary prism. Site 542 terminated in the frontal thrust where the major displacement on the décollement propagates upward to the deformation front. By attempt-

ing to place Site 675 west of this location we hoped to test only the décollement and avoid the complication of its intersection with the frontal thrust.

The principal objectives of Site 675 were as follows:

1. To determine the fluid pressure and *in-situ* permeability in the décollement zone.
2. To collect a suite of logs across the décollement to determine physical properties *in situ*.
3. To collect an additional suite of cores across the décollement and define its geochemical and structural characteristics at a location close to the deformation front.

OPERATIONS

One hole was drilled at Site 675, located about 2 km west of the Barbados Ridge deformation front and approximately 400 m west of DSDP Hole 542. Site 675 was approached by dead reckoning navigation as the GPS navigation system was not working. The beacon was dropped at 1115 hr, 3 August 1986, and drill pipe was being tripped when the transit satellite system indicated that the ship was 2 mi north of the intended drill site. The ship was offset 2 mi south utilizing the Site 671 beacon, still working after 40 days, for baseline. After the final position was verified, a new beacon was dropped and the vessel offset 50 m. The location of Site 675 is 15°31.77' N, 58°43.01' W, in 5008.1 m of water.

The primary objective of Hole 675A was to drill to the décollement and test the formation with a packer, the Retrieval Formation Tester (RFT—also called an open hole packer). The drill-

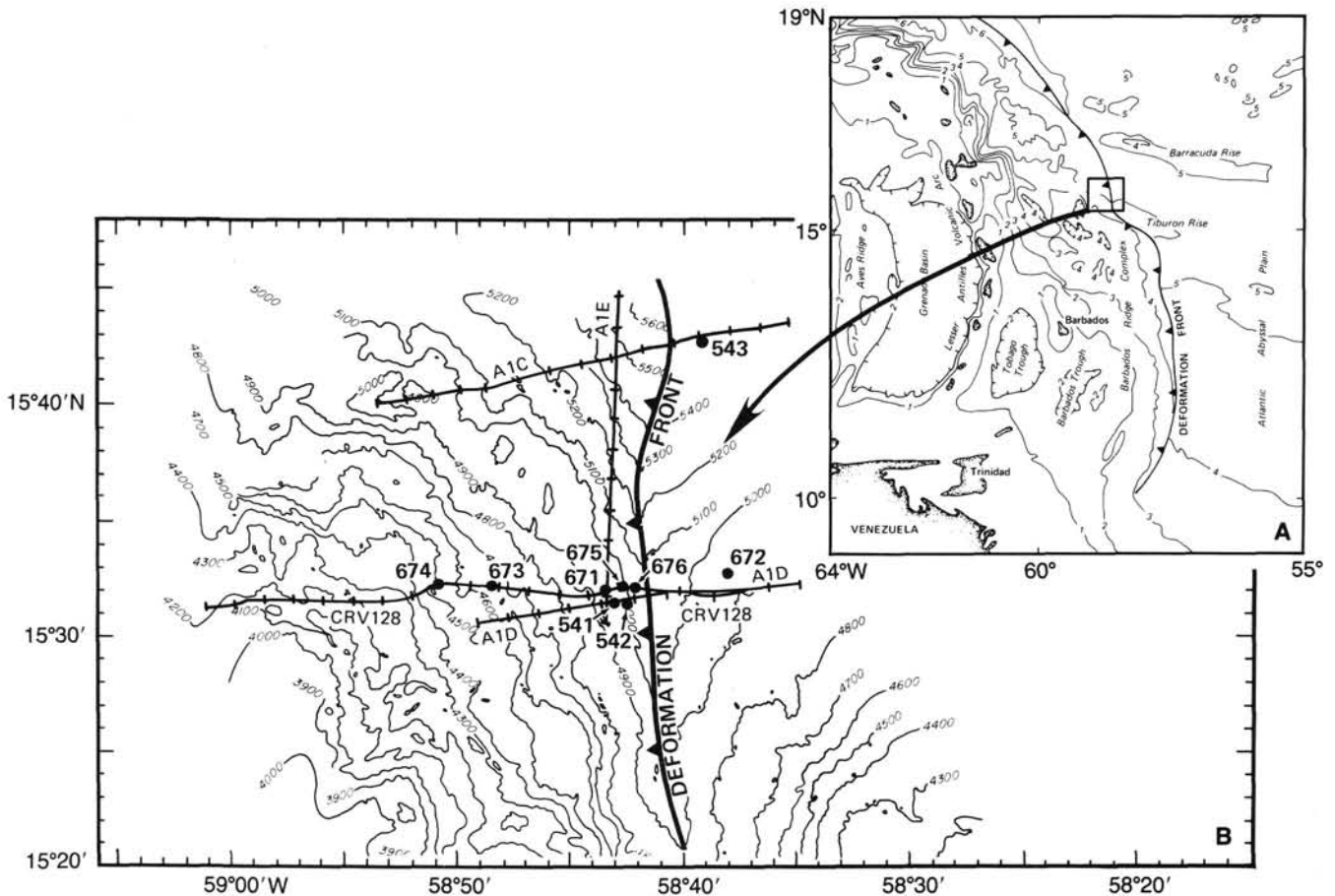


Figure 1. A. General location map of leg 110 drilling area. B. Legs 78A and 110 drill site locations.

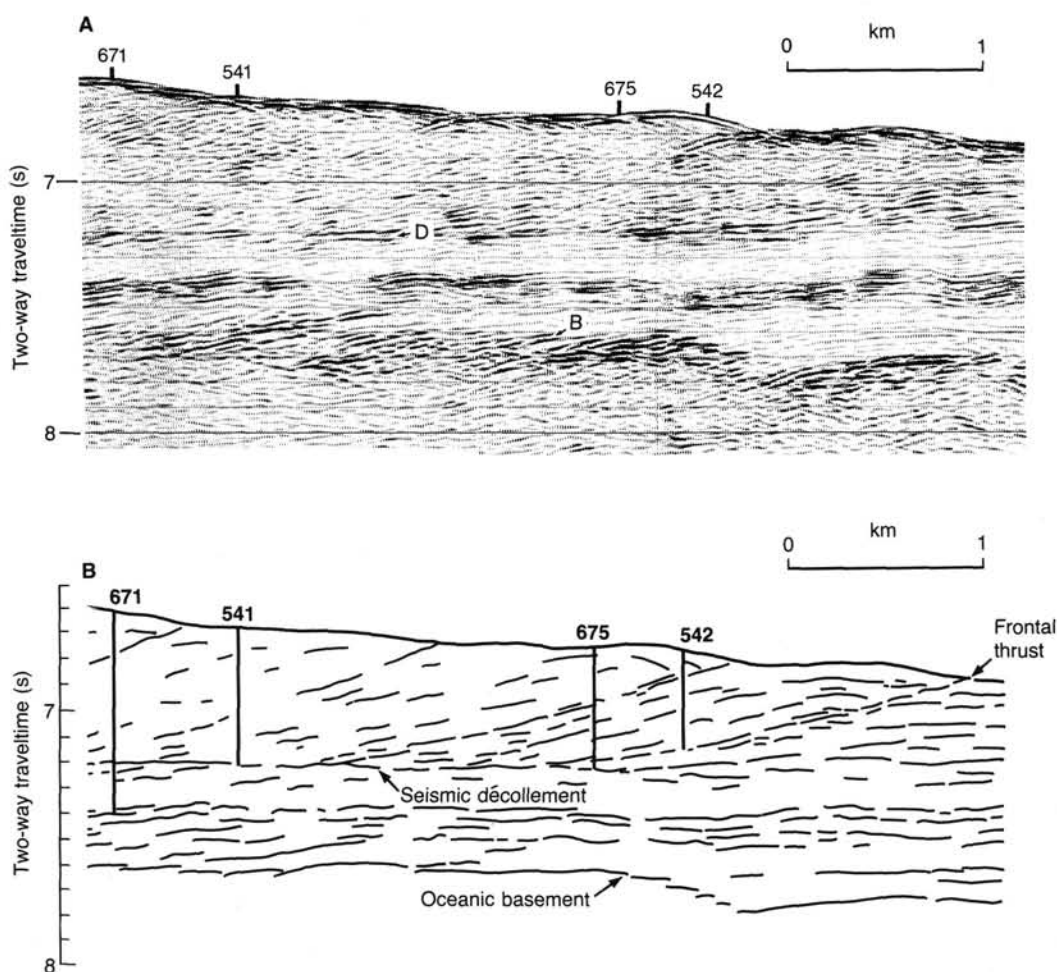


Figure 2. Migrated seismic section and line drawing of eastern extent of Barbados Ridge complex along Leg 110 transect. A: Uninterpreted time section, CRV 128. Reflector "D" is seismic décollement. Reflector "B" is top of oceanic basalt. Vertical exaggeration is 1.7:1 at water bottom. B: Line drawing interpretation of A showing extrapolated depth of Sites 671, 541, 675, and 542.

ing operation utilized an XCB bit, a six-drill-collar BHA, a 10½" bit and sufficient pump to clean the hole without eroding the well bore.

The drill string was tripped to the seafloor PDR-indicated depth of 5004.3 m. This depth was suspect because three distinct bottoms were visible on the records. After one water core, a 22-cm recovery in Core 110-675A-1H established the mudline at 5018 m of drill pipe. The hole was drilled as planned but conditions deteriorated as the well was deepened. Three to five meters of fill were common on each connection. Cores 110-675A-2X through -8X were recovered between 321.6 and 388.1 mbsf. The total cored interval in Hole 675A was 66.7 m, of which 44.7 m of sediment were retrieved, a 67% recovery rate. Torque increased in the bottom of the hole and the cores indicated that the décollement had been crossed without finding a suitable packer seat. The last three cores were drilled in 3 min of rotating time. The hole conditions on the last cores were noted as follows:

1. A dramatic increase in rate of penetration.
2. Porosity values in the last core that were approximately the same as extrapolated porosities in the upper 50 m of the hole.
3. Drill string torque was increasing. Overpulls of 20 to 30 thousand pounds were required to move the drill pipe because of the sticky hole conditions.

These conditions are similar to the drilling conditions reported at DSDP Site 542.

The softness of the formation at or above the zone of interest precluded the use of open hole packers. The scientific party elected to abandon the hole and move back upslope to Site 671 where the formation might provide a better packer seat. The hole was filled with heavy mud and drill string retrieved. Table 1 summarizes the coring at Site 675. The ship moved off location at 2145 hr on 6 August 1986 after 3.1 days of operation.

STRUCTURAL GEOLOGY

Hole 675A was washed to 321.6 mbsf after only recovering a 20-cm-long mudline core. The structural data obtained from Cores 110-675A-2X to -8X contain potentially valuable information about the basal décollement of the Lesser Antilles accretionary prism. No relevant data on the décollement had been gained in the previous drilling of DSDP Site 542 on Leg 78A (Biju-Duval, Moore et. al, 1984b), as the drill hole had to be abandoned at 325.5 mbsf in the frontal thrust.

The first indications of sediment deformation in this hole are in Core 110-675A-3X, in the form of two brittle faults with dips of about 45°, and two distinct zones of scaly fabrics in claystones (Fig. 3). The dip of the scaly fabrics is also about 45°. Cores 110-675A-4X and -5X are essentially undisturbed. Core 110-675A-6X contains a wealth of small-scale structures. Scaly fabrics occur throughout this core (Fig. 3) with dips varying be-

Table 1. Coring summary, Site 675.

Core 110-675A-	Date Aug. 1986	Time	Sub-bottom top (m)	Sub-bottom bottom (m)	Meters cored (m)	Meters recovered (m)	Percent recovery
1H	4	0720	0.0	0.2	0.2	0.22	110.0
2X	5	1341	321.6	331.1	9.5	5.87	61.8
3X	5	1600	331.1	340.6	9.5	3.49	36.7
4X	5	1800	340.6	350.1	9.5	6.25	65.8
5X	6	0335	350.1	359.6	9.5	9.73	102.0
6X	6	0545	359.6	369.1	9.5	9.19	96.7
7X	6	0820	369.1	378.6	9.5	0.52	5.5
8X	6	1110	378.6	388.1	9.5	9.47	99.7
					66.7	44.74	

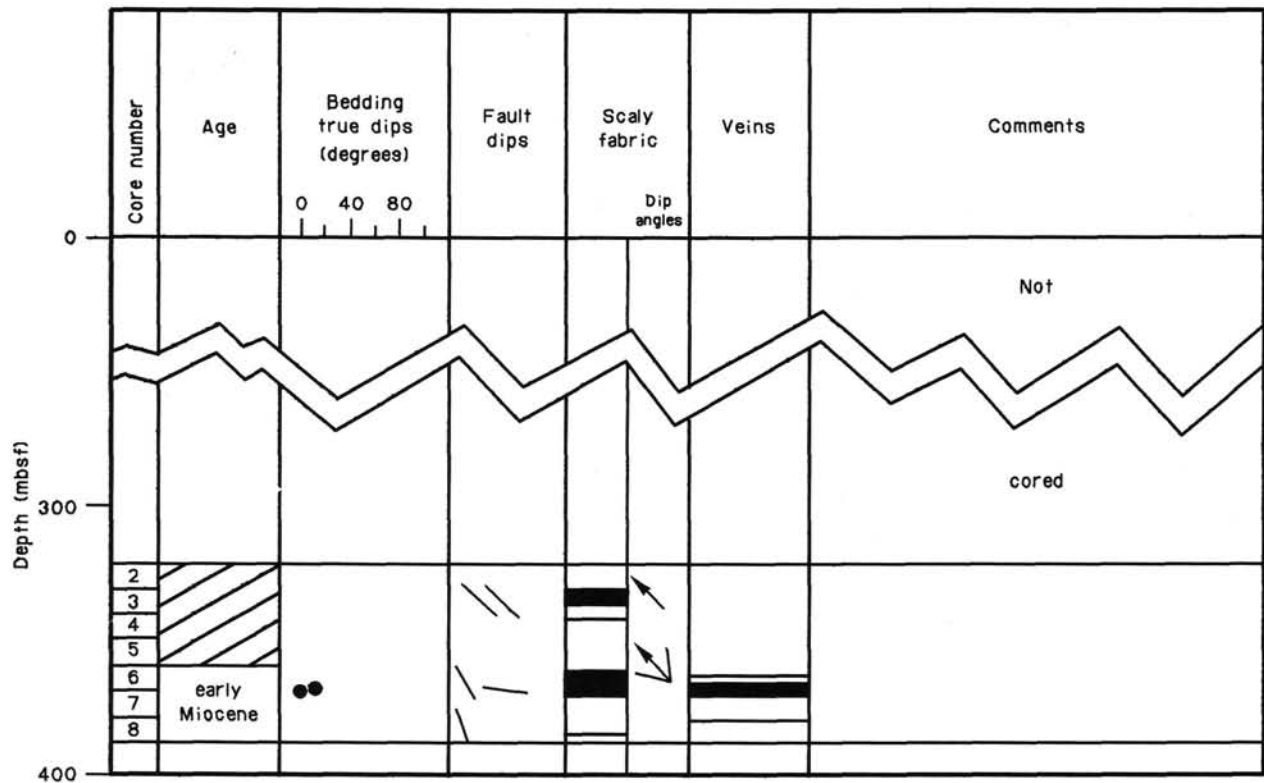


Figure 3. Structural log of Hole 675A. The dip of scaly cleavages is indicated by a range (the angle encompassed by the two bars) and dominant dip (bar with arrowhead). For discussion see text.

tween 20 and 80°, but with a clear maximum at about 50°. Centimeter-sized veinlets filled with rhodochrosite (Fig. 4), which in places overprint the scaly fabric, are found in Core 110-675A-6X. These veinlets are subparallel to the scaly fabric, but in a few cases crosscut it at low angles. The dip of the veinlets is dominantly between 50° and 70°. One of the veins is cut off by a low-angle fault in Sample 110-675A-6X-6, 66–75 cm, and another one (Sample 110-675A-6X-3, 142–147 cm) was found to have a surface with dip-slip slickensides, documenting that there was some shear displacement parallel to the vein boundary. These findings constrain an evolutionary path of tectonic structures from scaly fabric formation to dilatant veining with accompanying and postdating brittle shearing. Recovery in Core 110-675A-7X was extremely poor, so that no inferences can be made about the exact footwall depth of this zone of deformation. The lack of recovery may indicate that this is in fact the most deformed and disaggregated part of the log. No more structures except for one high-angle brittle fault, a set of clay-filled veins (Sample 110-675A-8X-1, 95–101 cm), and one thin band of scaly

fabrics were encountered in Core 110-675A-8X, indicating that the footwall of deformation is somewhat higher up in the section. Information about orientation of bedding planes is restricted to Core 110-675A-6X, where the planes are more or less horizontal.

In summary, two well-defined zones of tectonic deformation were intersected in Hole 675A. The upper one (Fig. 3) at about 335 mbsf may correspond to the deformation related to the frontal thrust of the Lesser Antilles accretionary prism. The lower zone of deformation between 360 and 378 mbsf then corresponds to the seaward propagating basal décollement. Note that displacements in this frontal location are not large. Therefore it is not surprising to find a smaller volume of rock deformed in association with thrusting, if compared to the structures encountered in Hole 671B (this volume). The veining gives evidence that, at least in the late (Holocene) part of its structural history, the basal décollement hosted fluid pressures close to the lithostatic head to allow tensional dilatant failure and crack-sealing in the scaly claystones.

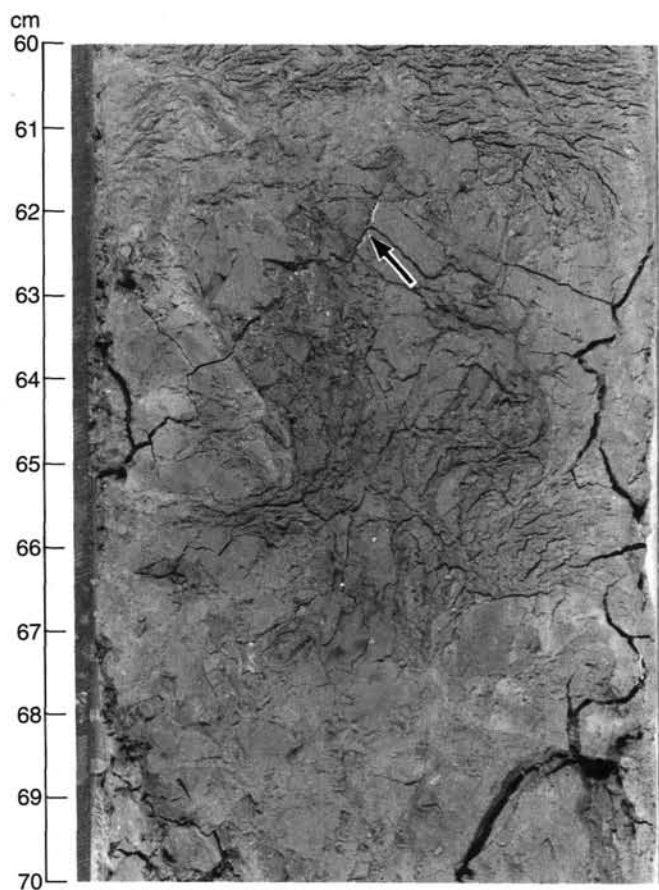


Figure 4. Close-up photograph of Core 110-675A-6X-4, 60–70 cm, showing incipient scaly fabrics distorted by drilling, and a small whitish rhodochrosite veinlet (arrow). The conjugate fracture sets near the veinlets probably result from axial loading of the core during drilling.

LITHOSTRATIGRAPHY

Sediment Lithology: Description

The sediments recovered at Site 675 are divided into three units on the basis of visual core descriptions and smear-slide analyses (Table 2).

Unit 1

Only 22 cm of sediment were recovered. This unit consists of brown foraminifer-nannofossil ooze of early Pleistocene age. Unit 1 is separated from Unit 2 by a 321.4-m-thick washed interval extending from 0.2 to 321.6 mbsf.

Unit 2

This unit is 41.91 m thick, barren of microfossils, and thus of indeterminate age. Although the unit extends from 321.6 to 363.5 mbsf, much of the recovered interval consists of drilling breccia and hole-fill sediments that do not represent *in situ* lithologies. Those portions of the unit thought to be in place consist of moderately to highly bioturbated olive green-to-green mudstone and claystone. Burrows observed in this sequence are primarily *Planolites* and *Chondrites*. Unit 2 contains local minor dark gray ash. The lower boundary of the unit grades downward into Unit 3.

Unit 3

The unit extends from 363.5 mbsf to the base of Hole 675A at 388.1 mbsf. This unit consists of gradationally interlayered orange brown siliceous mudstone and nonsiliceous to slightly siliceous olive brown-to-olive mudstone. The orange brown portions of the unit, particularly the portion between 0 and 97 cm in Section 110-675A-8X-1, contain common black intervals (probably amorphous Mn-rich phases) and closely resemble the décollement horizon recovered at Site 671. Radiolarians recovered from this interval at Site 675 indicate an early Miocene age. Small (1 mm diameter) white spherules of clinoptilolite(?) are scattered throughout Unit 3, although they appear to be more common in the olive-colored, nonsiliceous intervals. The identification of these spherules as clinoptilolite is based on XRD analyses of similar spherules from the same stratigraphic interval at Site 671. Unit 3 sediments are locally slightly bioturbated.

All of the sediments recovered at Site 675 appear to be hemipelagic deposits. No current-related sedimentary structures occur in these units. The abundant carbonate microfossils preserved in Unit 1 indicate deposition of these sediments above the carbonate compensation depth (CCD). In contrast, the sediments of Units 2 and 3 contain no biogenic carbonate and thus were probably deposited below the CCD. The minor ash in Unit 2 probably represents air-fall deposition from the Lesser Antilles Arc. Although the sediments of Unit 2 are of indeterminate age, comparison with the reference lithologies from Site 672 suggests that these ash-bearing sediments are of Miocene age.

Bulk Mineralogy

Six samples from 324 to 385 mbsf at Site 675 were analyzed for bulk mineralogy (see Fig. 5). Methods are described in Chapter 1. These samples are all from Lithologic Units 2 and 3, are barren or of early Miocene age, and have mineralogical compositions similar to Miocene sediments recovered at previous sites. The sediments are calcite-free and contain approximately 70%–90% total clay minerals, 5%–20% quartz, and 2%–26% plagioclase.

Table 2. Lithologic units at Site 675.

Unit	Lithology	Core range (core-section, cm level)	Depth (mbsf)	Age
110-675A-				
1	Brown foraminifer-nannofossil marly ooze	1H-CC	0.0–0.22	Early (?) Pleistocene
2	Olive green to green mudstone and claystone	2X-1 to 6X-3, 91 cm	321.6–363.5	Indeterminate
3	Interlayered orange brown siliceous mudstone and olive to olive brown nonsiliceous to slightly siliceous mudstone	6X-3, 91 cm to 8X-CC	363.5–388.1	Early Miocene and indeterminate

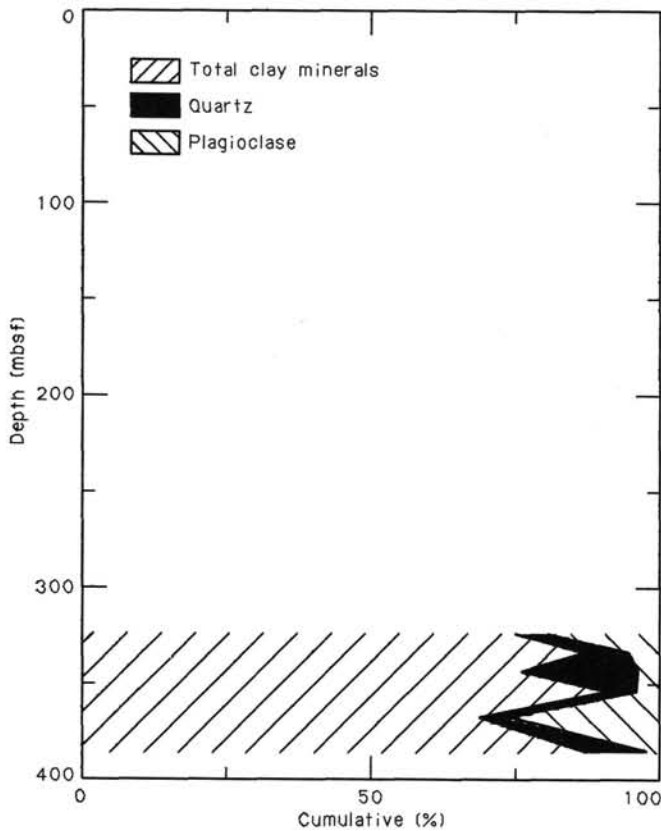


Figure 5. Bulk mineralogy of Site 675 samples expressed as cumulative percentages of total clay minerals, quartz, plagioclase, and calcite.

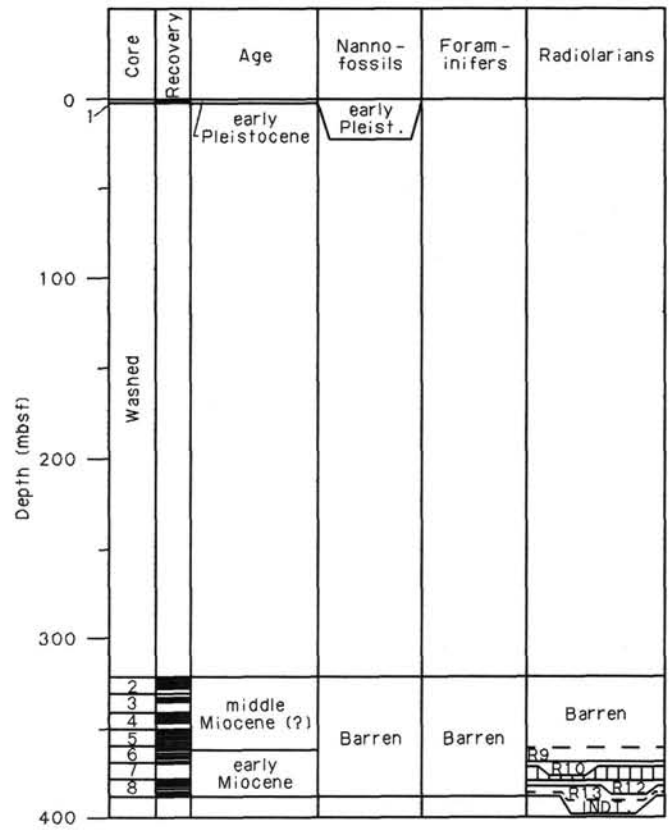


Figure 6. Site 675 biostratigraphic summary. R9: *Calocycletta costata* Zone, R10: *Stichocorys wolffii* Zone, R12: *Cyrtocapsella tetrapera* Zone, R13: *Lychnocanoma elongata* Zone.

BIOSTRATIGRAPHY

Summary

At Site 675, one mudline core and 66.5 m of sediments below 321.4 mbsf have been recovered. The uppermost sediments (Core 110-675A-1H) are Pleistocene in age based on calcareous nanofossils.

Cores 110-675A-2X through -8X are barren of calcareous microfossils, and Cores 110-675A-2X through -5X are also barren of radiolarians.

Sediments from 365 to 384 mbsf (Samples 110-675A-6X-4, 76-78 cm through -8X-4, 50-52 cm) are assigned to the lower Miocene on the basis of radiolarians. A missing section, marked by the absence of the *S. delmontensis* Zone and the lower and middle parts of the *S. wolffii* Zone, is suspected in the middle part of this interval (Fig. 6). Poor recovery in Core 110-675A-7X may be responsible for this biostratigraphic gap.

Based on superposition, sediments cored above 363 mbsf and below 385 mbsf are regarded as middle Miocene and earliest Miocene (or latest Oligocene) in age, respectively, although no age indicators occur in these horizons.

Calcareous Nanofossils

No calcareous nanofossils are preserved in Cores 110-675A-2X through -8X. The mudline core is early Pleistocene in age, based on the presence of *Pseudoemiliana lacunosa* and *Calcidiscus macintyreii* without *Discoaster brouweri*. Pliocene reworking is common in this sample.

Planktonic Foraminifers

No foraminifers are preserved in sediments cored at Site 675.

Radiolaria

Radiolarians occur in samples below Sample 110-675A-6X-4, 76-78 cm, and are absent in samples above Sample 110-675A-6X-3, 76-78 cm (Table 3). Core 110-675A-1H was not examined.

Sediments between Samples 110-675A-6X-4, 76-78 cm and -6X-CC, 27-34 cm are assigned to the *Calocycletta costata* Zone (Riedel and Sanfilippo, 1978) because of the presence of *C. costata*, *Dorcadospyris dentata*, and *Liriospyris stauropora*, and the absence or rare occurrence of *Dorcadospyris alata*. Although Sample 110-675B-6X-4, 76-78 cm contains few and poorly preserved radiolarians, it is placed within the range of *C. costata* owing to the presence of this taxon. This interval is assigned to the *C. costata* Zone because: a) all specimens of *Dorcadospyris* which occur in this sample are close to *D. dentata* and b) the biozonal assignment of the sample immediately underneath (Sample 110-675A-6X-5, 76-78 cm) is still in the middle part of the *C. costata* Zone. Radiolarians are common to abundant and preservation is moderate to good in Samples 110-675A-6X-5, 76-78 cm through -6X-CC, 27-34 cm.

Sample 110-675A-7X-CC, 16-23 cm is assigned to the upper part of *Stichocorys wolffii* Zone (Riedel and Sanfilippo, 1978) because of the presence of *Stichocorys delmontensis*, *S. wolffii*, *L. stauropora*, and *D. dentata*, and the absence of *C. costata* and *D. alata*.

Samples 110-675A-8X-1, 8-10 cm through -8X-2, 148-150 cm are assigned to the *Cyrtocapsella tetrapera* Zone (Riedel and Sanfilippo, 1978) because of the presence of *Cyrtocapsella cornuta*, *C. tetrapera*, *Carpocanopsis cingulata*, and *Dorcadospyris ateuchus*, and the absence of *S. delmontensis*, *S. wolffii*, and *Carpocanopsis bramlettei*. In Samples 110-675A-8X-1, 102-104 cm through -8X-2, 100-102 cm, *Calocycletta serrata* is common.

Table 3. Abundance, preservation, and biostratigraphic horizon of radiolarians in Hole 675A.

Sample 110-675A	Abundance Preservation	Zone	Age
-2X-CC, 19-22 cm	B		?
-3X-CC, 8-14	B		?
-4X-CC, 1-8	B		?
-5X-CC, 29-36	B		?
-6X-1, 76-78	B		?
-6X-2, 76-78	B		?
-6X-3, 76-78	B		?
-6X-4, 76-78	FP	R9+R8-4 (<i>C.c</i> + <i>D. alata</i>)	e. Miocene
-6X-5, 76-78	AM	R9-2: <i>C. costata</i> Z.	e. Miocene
-6X-6, 76-78	AM	R9-2: <i>C. costata</i> Z.	e. Miocene
-6X-CC, 27-34	AG	R9-3: <i>C. costata</i> Z.	e. Miocene
-7X-CC, 16-23	AG	R10-1: <i>S. wolffii</i> Z.	e. Miocene
-8X-1, 50-52	AM	R12-1: <i>C. tetrapera</i> Z.	e. Miocene
-8X-2, 50-52	AM	R12-2: <i>C. tetrapera</i> Z.	e. Miocene
-8X-3, 50-52	AP	R13: <i>L. elongata</i> Z.	e. Miocene
-8X-4, 50-52	AP	R13: <i>L. elongata</i> Z.	e. Miocene
-8X-5, 50-52	AvP	? (badly dissolved)	?
-8X-CC	AvP	? (badly dissolved)	?

A: abundant, C: common, F: few, B: barren
G: good, M: moderate, P: poor, vP: very poor

Appendix table showing the relation of "R" numbers.

-	Top: <i>C. costata</i>	<i>Dorcadospyrus alata</i> Zone
R8-a		
-----	<i>D. dentata</i> → <i>D. alata</i>	-----
R9-c		
-	<i>L. stauropora</i> → <i>L. parkerae</i>	
R9-b		<i>Calocyclus costata</i> Zone
-	Top: <i>C. cingulata</i>	
R9-a		
-----	Bottom: <i>C. costata</i>	-----
R10-c		
-	Bottom: <i>D. dentata</i>	
R10-b		<i>Stichocorys wolffii</i> Zone
-	Bottom: <i>L. stauropora</i>	
R10-a		
-----	Bottom: <i>S. wolffii</i>	-----
R11-b		
-	Top: <i>D. ateuchus</i>	<i>Stichocorys delmontensis</i> Zone
R11-a		
-----	Bottom: <i>S. delmontensis</i>	-----
R12-b		
-	Top:	
R12-a	<i>C. serrata</i>	<i>Cyrtocapsella tetrapera</i> Zone
-----	Bottom: <i>C. tetrapera</i>	-----
R13		<i>Lychnocanoma elongata</i> Zone
-----	Bottom: <i>L. elongata</i>	-----

Samples 110-675A-8X-3, 50-52 cm through -8X-4, 50-52 cm are assigned to the *Lychnocanoma elongata* Zone (Riedel and Sanfilippo, 1978). *L. elongata* and *C. cingulata* occur together with many specimens of *Calocyclus robusta* and the ancestral form of *Cyrtocapsella*. The terminal aperture of this species is wider than three times the distal pore diameter.

In sediments observed below Samples 110-675A-8X-4, 125-127 cm, radiolarians are abundant but badly dissolved. No age indicator was obtained.

The middle part of the *Stichocorys wolffii* Zone through the bottom of the *Stichocorys delmontensis* Zone of Riedel and Sanfilippo (1978) are missing, perhaps owing to the poor recovery in Core 110-675A-7X (5.5 %) and the above-mentioned probable hiatus.

PALEOMAGNETICS

There is no Paleomagnetism report for Site 675.

GEOCHEMISTRY

Introduction

Site 675 was drilled close to DSDP Site 542 of Leg 78A (Biju-Duval, Moore, et al., 1984b). The principal purpose of this hole was to carry out a packer experiment and to sample the zone of décollement for lithology and geochemistry. Unfortunately, as with its predecessor, hole conditions forced the abandonment of the site. This report briefly summarizes the results obtained and will draw upon information obtained in Site 542 (Gieskes et al., 1984) to suggest the possible geochemistry in the uncored section above 325 mbsf.

Results

The results are presented in Table 4 and in Figure 7.

Chloride

The chloride concentrations show strong variability with depth, suggesting the presence of fault zones above the actual décollement, much the same as at Site 671. Indeed, hole conditions were lamentable, especially near Cores 110-675A-6X and -7X, probably related to zones of potential movement of low-salinity waters. The data strongly suggest that coring started in or very near a major fault zone. We present below the data on methane which also suggest this.

Calcium and Magnesium

The data of Figure 7 suggest that indeed Hole 542 can, as a first approximation, be considered as a precursor of Hole 675A. This is so notwithstanding the distance of about 1200 m between the sites. The data suggest that in this area at least a certain lateral heterogeneity exists in calcium and magnesium profiles above the décollement zone. Perhaps the termination of Hole 542 was caused by a cave-in associated with a fault above the décollement similar to the situation here.

The calcium and magnesium profiles show distinct gradients toward the décollement, with the magnesium gradient being quite similar to that observed directly above the décollement of Site 671.

Sulfate and Ammonia

The data on sulfate and ammonia for Hole 542 are not of sufficient quality for an adequate comparison. However, dissolved SO_4^{2-} is lower at Site 675 (Table 4) than in the décollement zone of Site 671, and similarly NH_4^+ concentrations are higher (Table 4). This may well be related to the higher rates of sedimentation in the upper part of hole 675; note that Site 542 has a much higher sedimentation rate than Site 671. These differences are probably related to structural complications in both holes.

Silica

Concentrations of dissolved silica are particularly high in Cores 110-675A-6X and -8X, i.e., in the zones rich in radiolarians. Silica in Core 110-675A-8X is typical for the yellowish sediments associated with the décollement of Sites 671 and 672 (future décollement). Higher values of silica also occur in barren Core 110-675A-2X; this may be related to a possible nearby fault.

Conclusions

Evidence from chloride, calcium, and magnesium concentration-depth profiles suggests that the first deep core at Site 675 was in or close to a fault zone through which advection of low-chlorinity fluids is occurring, either presently or in the very recent past. In addition, the geochemical data at this hole show

Table 4. Geochemistry data, Site 675, with chlorine, calcium, and magnesium data for Sites 542 and 542A.

Core 110-675A-	Sec.	Int. (cm)	Depth (mbsf)	pH	Alkalinity (mmol/L)	Salinity ‰	Cl (mmol/L)	Ca (mmol/L)	Mg (mmol/L)	NH ₄ (μmol/L)	Si (μmol/L)	SO ₄ (mmol/L)
2	2	145-150	325	—	—	30.0	500	42.4	27.7	450	490	14.0
3	2	145-150	334	—	—	32.3	537	44.6	29.2	390	250	15.6
4	3	145-150	345	—	—	32.0	527	38.5	32.7	425	190	17.8
5	3	145-150	355	7.86	1.02	32.0	531	41.4	32.8	580	200	15.6
6	5	145-150	366	—	—	31.5	512	38.5	34.1	520	960	15.3
8	4	145-150	385	—	—	32.5	541	35.8	39.4	575	1015	14.4

Leg 78A Sites 542 and 542A

Core	Sec.	Int. (cm)	Depth (mbsf)	Cl (mmol/L)	Ca (mmol/L)	Mg (mmol/L)
Site 542						
H1	6	—	44 ± 44	563	12.0	48.5
H2	3	—	121 ± 33	562	30.0	29.9
H3	2	—	178 ± 24	563	37.0	25.2
Site 542A						
1	5	125-135	209	563	35.7	28.1
3	2	140-150	252	547	41.6	27.3
8	4	135-150	312	551	42.9	27.3

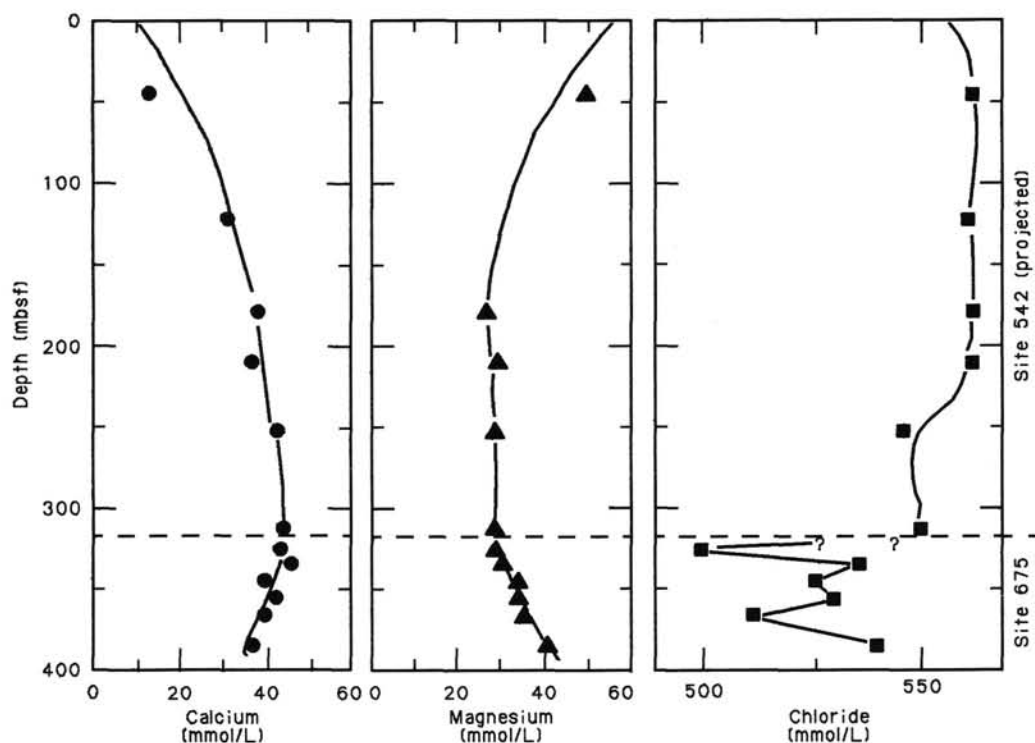


Figure 7. Calcium, magnesium, and chloride profiles, 0-322 mbsf at Site 542, and below 322 mbsf at Site 675.

evidence that coring ended very close to the bottom of the décollement zone.

Organic Geochemistry

The methane data for Site 675 are given in Table 5. The highest concentration of about 724 μmol/L (Fig. 8) corresponds with the lowest chloride content at 325 mbsf. As at Sites 671 and 672, we propose that methane is advected with low-chlorosity

waters along a major fault zone. At Site 675, this fault zone could belong to the frontal thrust system that emerges at the eastern edge of the Barbados Ridge complex. In accordance with methane data from Site 672, the increase of the methane concentration gradient from 334 mbsf to the bottom of Hole 675A indicates proximity to another high methane concentration zone. This zone probably represents the eastward propagating décollement described in Site 672.

Table 5. Rock-Eval data, organic carbon, inorganic carbon, and methane at Site 675.

Core 110-675A-	Sec.	Int. (cm)	Depth (mbsf)	Temp. (°C)	S ₁	S ₂	S ₃	PI	S ₂ /S ₃	PC	TOC (%)	HI	OI
2	2	145-150	325	467	0.16	1.57	0.11	0.09	14.27	0.14	0.14	1121	78
3	2	145-150	334	497	0.04	0.95	0.67	0.04	1.41	0.08	0.08	1187	837
4	3	145-150	345	459	0.04	1.14	0.28	0.03	4.07	0.09	0.09	1266	311
5	3	145-150	355	472	0.03	1.23	0.29	0.02	4.24	0.10	0.12	1025	241
6	5	145-150	366	461	0.03	0.98	0.32	0.03	3.06	0.08	0.08	1225	400
8	4	145-150	385	441	0.06	0.68	0.21	0.08	3.23	0.06	0.06	1133	350

Core 110-675A-	Sec.	Int. (cm)	Depth (mbsf)	Org. C %	Inorg. C %	CH ₄ (μmol/L)
2	2	145-150	325	0.14	0.05	724
3	2	145-150	334	0.08	0.02	307
4	3	145-150	345	0.09	0.03	317
5	3	145-150	355	0.12	0.05	n.d.
6	5	145-150	366	0.08	0.02	394
8	4	145-150	385	0.06	0.01	396

S₁ (mg hydrocarbon/g rock): the quantity of free hydrocarbons present in the rock and which are volatilized below 300°C.

S₂ (mg hydrocarbon/g rock): the amount of hydrocarbon-type compounds produced by cracking of kerogen as the temperature increases to 550°C.

S₃ (mg CO₂/g rock): quantity of CO₂ produced from pyrolysis of the organic matter in the rock.

S₂/S₃: A means of determining the type of organic matter in the rock.

— from 0.0 to 2.5: gas, type III

— from 2.5 to 5.0: oil/gas, type III

— from 5.0 to 10.0: oil, types I and II

Temperature (°C): maximum temperature at which maximum generation of hydrocarbon from kerogen occurs.

PI (Productivity Index): $PI = S_1/(S_1 + S_2)$.

PI characterizes the evolution level of the organic matter.

PC "Pyrolyzed carbon": $PC = k(S_1 + S_2)$ where $k = 0.083 \text{ mg C/g rock}$.

PC corresponds to the maximum quantity of hydrocarbons capable of being produced from the source rock given sufficient burial and time.

TOC: Total Organic Carbon

HI "Hydrogen Index": $HI = (100 \times S_2)/TOC$

OI "Oxygen index": $OI = (100 \times S_3)/TOC$

n.d. = not determined.

Rock-Eval Results

Similar to Sites 673 and 674, the total organic carbon (TOC) (Table 5) in Hole 675 is very low and quite constant (<0.15%) with depth. The organic matter in the Miocene-sampled series is residual.

PHYSICAL PROPERTIES

Introduction

Site 675 is located 1.25 km northwest of Site 542, the most easterly location within the accretionary prism sampled on Leg 110. The sediments sampled at this site are therefore the most recently influenced by the deformation front. The site objectives were to measure *in situ* fluid pressure and permeability with only minimal sampling for packer seat location. Consequently, the physical properties data collected at this site begin at a depth of 321 mbsf where the second core was taken. Index property and compressional velocity measurements were made on the collected samples.

Index Properties

Methods

The methods used to measure index properties are the same as described in Chapter 1. Measurements were not made in the first core because of small sample recovery (0.22 m).

Results

Although the dataset is small (Table 6), the index property measurements show two trends which generally follow the

changes described in lithologic Units 2 and 3. Unit 2 (321.6 to 363.5 mbsf) displays increasing porosity and water content with depth below seafloor and decreasing bulk density (Fig. 9). The grain density within Unit 2 varies between 2.62 and 2.88 g/cm³ (mean value = 2.71 g/cm³) and no consistent trend with depth.

Within lithologic Unit 3, the index properties reverse their trend with decreasing water content and porosity and increasing bulk density (Fig. 9). The grain density within this unit is lower with a mean of 2.66 g/cm³.

Discussion

A comparison of Site 675 data to the equivalent lithologic units at Sites 671 and 672 shows a consistent trend of index property data. Moving from west to east (Sites 671 to 672), the porosity increases within the equivalent lithologic zones (Fig. 10). Maximum and minimum porosity for each equivalent zone are as follows:

Site	Porosity (%)	
	Maximum	Minimum
671	65.8	47.7
675	70.7	58.0
672	80.5	62.6

It should be noted that the variation in porosity from site to site may also be attributed to gravitational consolidation and variations in sediment composition. The depths below seafloor of each equivalent zone are 456 mbsf for Site 671, 324 mbsf for Site 675 (which may not be the minimum), and 140 mbsf for Site 672.

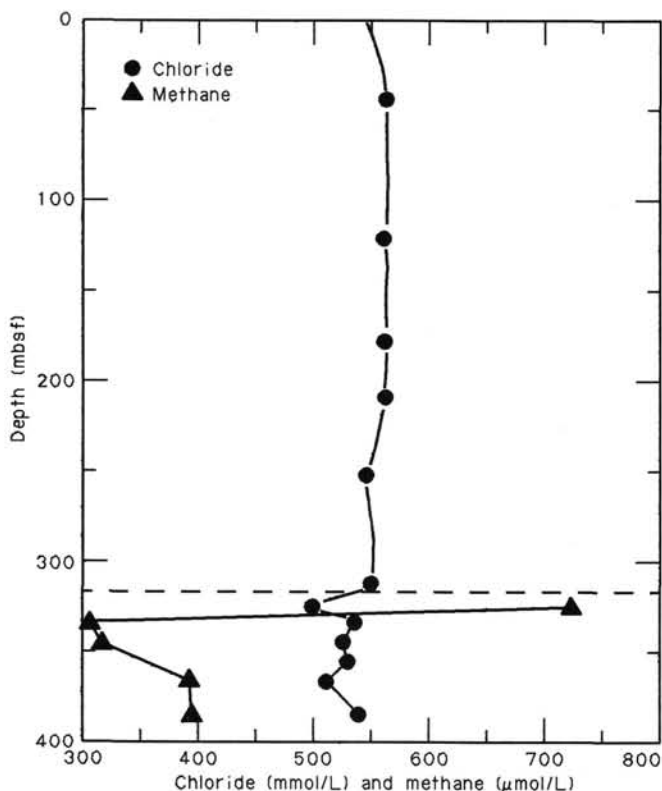


Figure 8. Methane and chloride profiles, Site 675. Chloride values above 322 mbsf are projected from Site 542.

Compressional Wave Velocity

Methods

Refer to Chapter 1 for a description of the methods used to measure compressional wave velocity. At Site 675 the Hamilton Frame method was used. Measurements were not made on Core 110-675A-1H (mudline) owing to minimal sample recovery.

Results

Within lithologic Unit 2, the velocity data show some scatter (Fig. 9). The velocity maximum and minimum within this unit are 1.73 and 1.55 km/s, respectively. Measurements made parallel to the core axis are not significantly different from those made perpendicular to the core axis (Table 7).

The four Unit 3 velocity measurements show a slight increase with depth below the seafloor from 1.62 to 1.68 km/s (Fig. 9).

Discussion

The compressional wave velocity measurements made at Site 675 reflect the relatively high water content of the sediment and correlate with the sediments sampled at Sites 671 and 672 where the pore-fluid space dominates the velocity of the matrix (refer to Fig. 39, Site 672 chapter).

Summary

Although the sampled interval at Site 675 is small, it serves to highlight the variation in consolidation characteristics of the lower Miocene clays (décollement zone) both within the accretionary prism (Sites 671 and 675) and outside the prism (Site 672). A systematic porosity and water content increase within these lithologic units is seen among Site 671, Site 675, and Site 672. This increase also corresponds to a shallowing of the zone from 456 mbsf at Site 671 to 160 mbsf at Site 672 and an increasing distance seaward of the thickest and first-deformed sediments of the accretionary prism.

SEISMIC STRATIGRAPHY

Site 675, located at shotpoint 370 on seismic line CRV 128, falls between the projections of Sites 541 and 542 on this line. The hole was only cored at the mudline (20 cm) and from 321 to 388 mbsf; velocity measurements from this interval were linearly projected to the surface with an inferred average velocity for the entire section of 1.58 km/s. This average was adjusted to *in-situ* conditions using a 2% increase, based on a comparison of logging and core measurements at Site 672. Accordingly, the estimated average velocity at Site 675 is 1.61 km/s. Although this velocity is low, it is consistent with the minimal decrease in porosity observed at Site 675 relative to Site 672 (see Physical Properties, this chapter).

At shotpoint 370 on CRV 128, the décollement occurs at 490 ms, which translates into a depth of 395 mbsf (Fig. 2). This décollement depth agrees reasonably with the stratigraphically defined lower Miocene décollement that probably lies in a zone of no recovery at 369 to 379 mbsf. The deformation zone observed at about 335 mbsf in barren, but probably middle Miocene, sediments may correlate with the frontal thrust at about 450 ms (inferred depth of 362 mbsf at 1.61 km/s) (Fig. 2). Thus the seismic data predicts both the décollement and the frontal thrust to be at greater depths than were observed by drilling. These systematic differences are probably owing to small irresolvable errors in location and or resolution of the seismic line.

Table 6. Index property measurements, Hole 675A.

Core 110-675A-	Sec.	Int. (cm)	Depth (mbsf)	% Water (wet)	% Water (dry)	Porosity %	Bulk density	Grain density
2	2	130	324.40	36	56	61.7	1.75	2.71
2	4	80	326.90	36	56	60.7	1.72	2.67
3	1	123	332.33	36	56	65.2	1.85	2.69
3	2	110	333.70	37	58	62.1	1.73	2.69
4	1	36	340.96	41	68	65.8	1.66	2.70
4	4	13	345.23	42	72	67.5	1.66	2.72
5	1	21	350.31	45	83	70.7	1.60	2.62
5	3	57	353.67	39	65	67.2	1.75	2.88
5	6	114	358.74	41	69	66.8	1.68	2.72
6	2	22	361.32	41	71	66.4	1.64	2.74
6	5	104	366.64	39	63	64.0	1.69	2.66
6	6	83	367.93	39	65	65.2	1.70	2.66
8	1	14	378.74	37	60	62.4	1.71	2.63
8	3	57	382.17	35	53	59.7	1.76	2.63
8	4	120	384.30	34	51	59.0	1.78	2.63
8	6	76	386.86	32	47	58.0	1.86	2.75

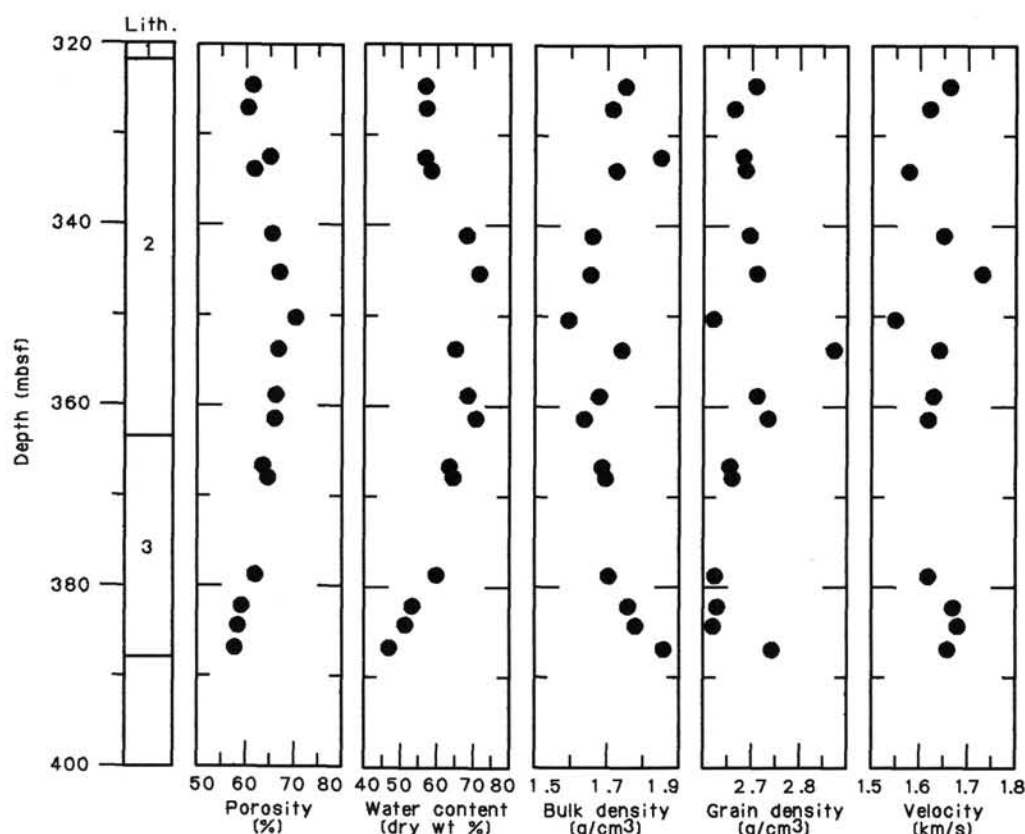


Figure 9. Porosity, water content, bulk density, grain density, velocity, and lithology vs. depth below seafloor for Hole 675A.

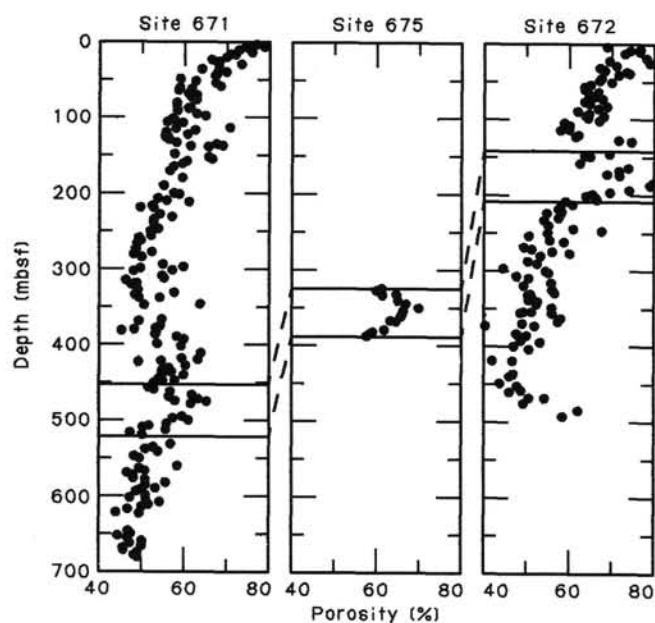


Figure 10. Porosity vs. depth below seafloor for Sites 671, 675, and 672.

HEAT FLOW

There is no Heat Flow report for Site 675.

SUMMARY AND CONCLUSIONS

As Site 675 was drilled specifically to set the drill-in packer, coring was minimal. A surface core, recovering only 22 cm,

Table 7. Compressional wave velocity measurements.

Core	Sec.	Int. (cm)	Depth (mbsf)	Vel (A)* (km/s)	Vel (B)* (km/s)
2	2	130	324.40	1.64	1.66
2	4	80	326.90	1.62	1.62
3	2	110	333.70	1.62	1.58
4	1	36	340.96	1.58	1.65
4	4	13	345.23	1.70	1.73
5	1	21	350.31		1.55
5	3	57	353.67		1.64
5	6	114	358.74		1.63
6	2	22	361.32		1.62
8	1	14	378.74	1.66	1.62
8	3	57	382.17	1.62	1.67
8	4	120	384.30	1.64	1.68
8	6	76	386.86	1.62	1.66

*Vel (A): velocity measured parallel to core axis
 Vel (B): Velocity measured perpendicular to core axis.

consists of lower Pleistocene foraminifer-nannofossil ooze (Unit 1). After the drilling washed to 321 mbsf, coring resumed until 388 mbsf, recovering 42 m of barren mudstone and claystone (Unit 2), and 25 m of locally siliceous lower Miocene mudstone (Unit 3; Fig. 11). Orange brown portions of Unit 3 with black manganese concentrations (especially Section 110-675A-8X-1) lithologically resemble the top of the décollement zone at Site 671. The lower Miocene radiolarian zones (R-10 through R-12) in Cores 110-675A-7X and -8X also correlate well with the top of the décollement zone at Site 671 (see Biostratigraphy section, this chapter). This litho- and biostratigraphic identification of the top of the décollement zone is close to the predicted depth of the seismic décollement.

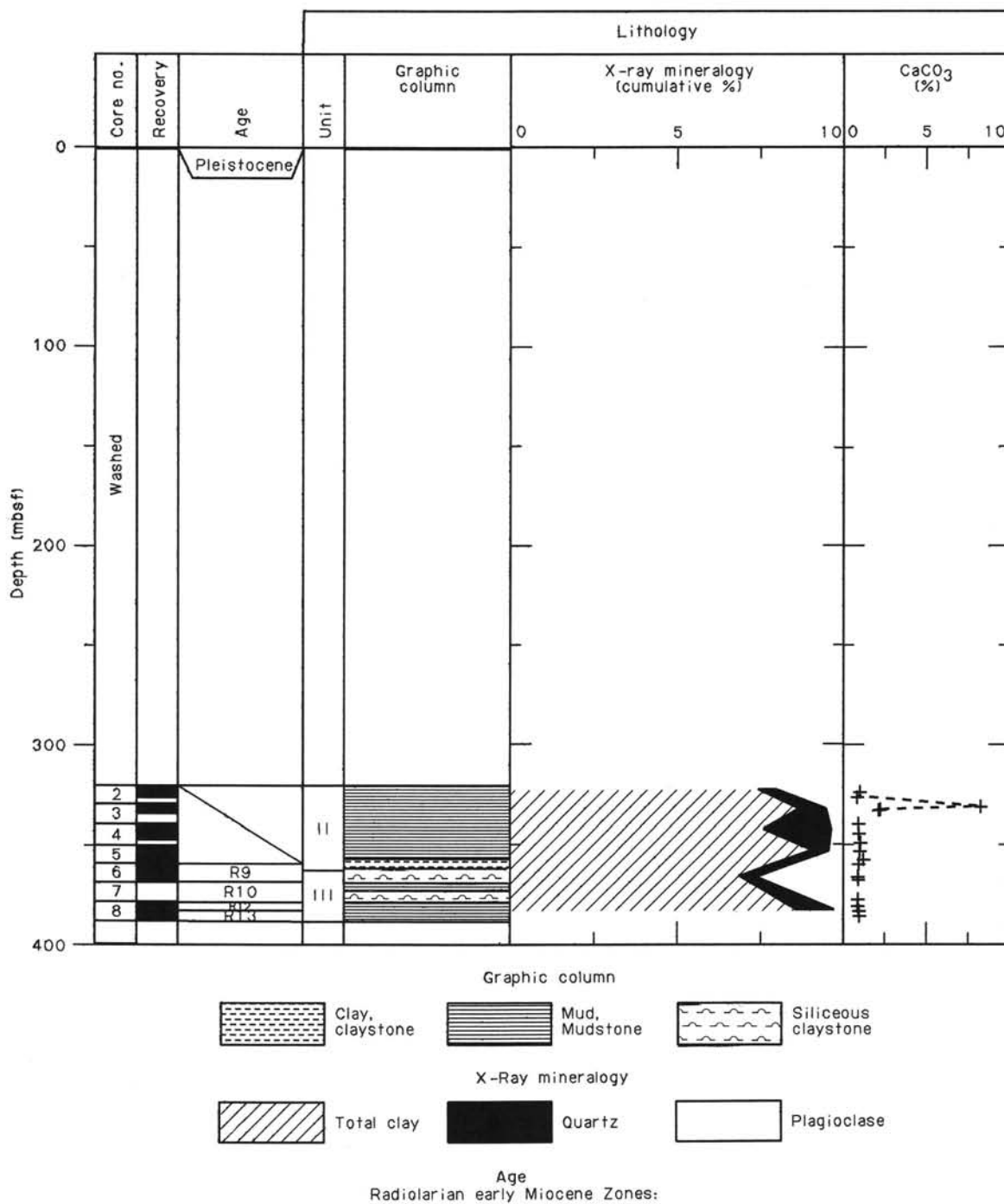


Figure 11. Site 675 summary diagram.

At Site 675 prominent zones of scaly fabric occur at about 335 mbsf and 360 to 378 mbsf (Fig. 11). The latter interval corresponds well to the stratigraphically inferred top of the décollement zone, whereas the former may correlate with a thrust splaying off the décollement zone. Pore-water chemistry results show a pronounced chloride low and methane high near the deformation zone at 335 mbsf, suggesting that the zone is active and perhaps part of the frontal thrust system (Fig. 11). A negative chloride anomaly and moderately elevated methane values in the lower deformation zone argue for active fluid flow. Rhodochro-

site occurs in shear veins lying in, and dilatant veins cutting across, the scaly fabric of the lower deformation zone. Near-lithostatic fluid pressures must have been present to open the veins for mineral precipitation during and after the development of the scaly fabric.

The porosity values from Site 675 show a high at about 350 mbsf. This positive excursion correlates with porosity highs in biostratigraphically equivalent cores just above both the décollement zone at Site 671 and the predicted future décollement zone at Site 672. The mean porosity of this lower Miocene zone

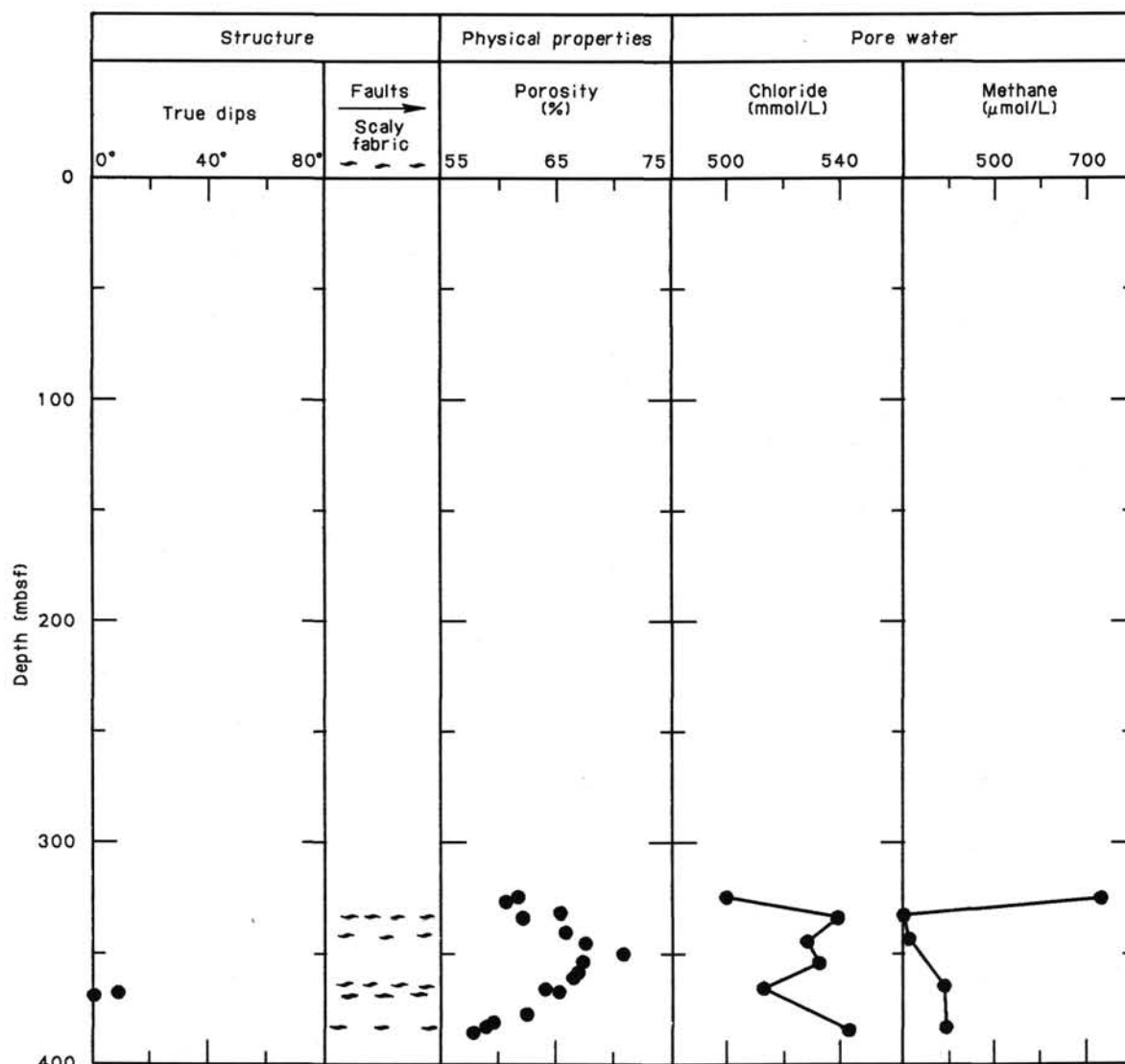


Figure 11 (continued).

drops from 69% at Site 672 to 61% at Site 675 to 58% at Site 671 (Fig. 10). A low estimated *in-situ* velocity of 1.61 km/s indicates that the sediments at Site 675 are not as consolidated as those further arcward at Sites 671, 673, and 674.

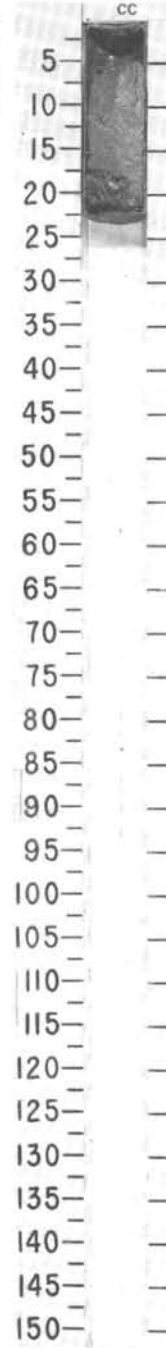
In summary, the pore-water chemistry, structural geology, and physical properties of cores from Site 675 all suggest active fluid movement at near-lithostatic fluid pressures. The relatively low state of consolidation and active dewatering of these materials obviated any packer experiment at this site but reflect the dynamic hydrologic system near the deformation front.

REFERENCES

- Biju-Duval, B., Moore, J. C., et al., 1984a. *Init. Repts. DSDP, 78A*: Washington (U.S. Govt. Printing Office).
- Biju-Duval, B., Moore, J. C., et al., 1984b. Site 542: Toe of the Barbados Ridge complex. In Biju-Duval, B., Moore, J. C. et al., *Init. Repts. DSDP, 78A*: Washington (U.S. Govt. Printing Office), 187-225.
- Bray, C. J., and Karig, D. E., 1985. Porosity of sediments in accretionary prisms and some implications for dewatering processes. *J. Geophys. Res.*, 90: 768-778.
- Gieskes, J. M., Elderfield, H., Lawrence, J. R., and LaKind, J., 1984. Interstitial water studies, Leg 78A. In Biju-Duval, B., Moore, J. C. et al., *Init. Repts. DSDP, 78A*: Washington (U.S. Govt. Printing Office), 377-384.
- Larue, D. K., Schoonmaker, J., Torrini, R., Lucas-Clark, J., Clark, M. and Schneider, R., 1985. Barbados: maturation, source rock potential and burial history within a Cenozoic accretionary complex. *Mar. Petrol. Geol.*, 2: 96-110.
- Marlow, M. S., Lee, H. and Wright, A., 1984. Physical properties of sediment from the Lesser Antillies Margin along the Barbados Ridge: results from Deep Sea Drilling Project leg 78A. In Biju-Duval, B., Moore, J. C., et al., *Init. Repts. DSDP, 78A*: Washington (U.S. Govt. Printing Office), 549-558.
- Masle, A., Biju-Duval, B., De Clarens, Ph. and Munsch, H., 1986. Growth of accretionary prism, tectonic processes from Caribbean examples. In Wezel, D. (Ed.), *The origin of arcs*: Amsterdam (Elsevier Scientific), 375-400.
- Riedel, W. R., and Sanfilippo, A., 1978. Stratigraphy and evolution of tropical Cenozoic radiolarians. *Micropaleontology*, 24: 61-96.
- Stride, A. H., Belderson, R. H., and Kenyon, N. H., 1982. Structural grain, mud volcanoes and other features on the Barbados Ridge complex revealed by GLORIA long-range side-scan sonar. *Mar. Geol.*, 49: 187-196.
- Westbrook, G. K., and Smith, M. J., 1983. Long décollements and mud volcanoes: Evidence from the Barbados Ridge Complex for the role of high pore-fluid pressure in the development of an accretionary complex. *Geology*, 11:279-283.

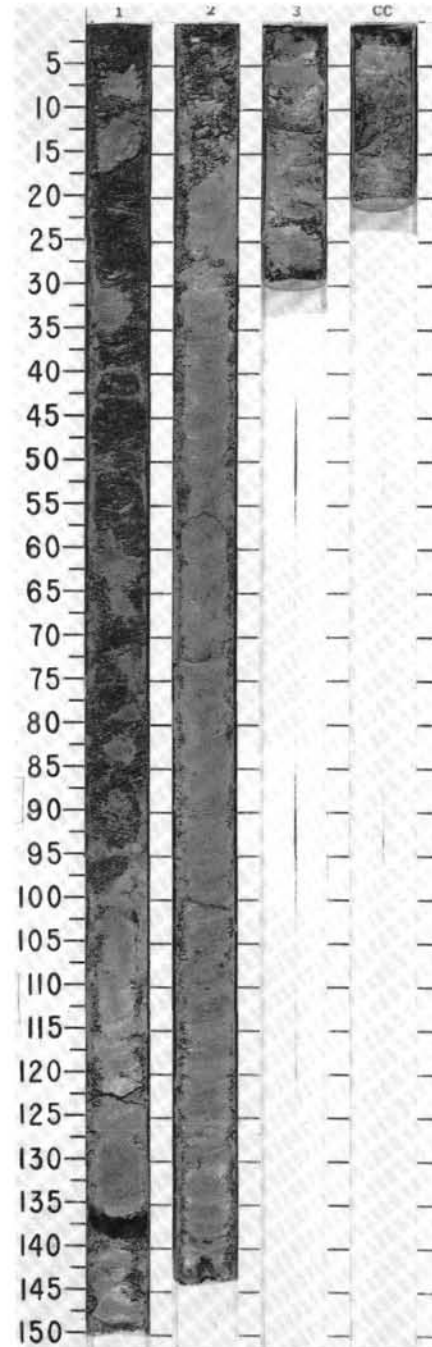
SITE 675 HOLE A CORE 1 H CORED INTERVAL 5008.1-5008.3 mbsl; 0.0-0.2 mbsf

TIME-ROCK UNIT	BIOSTRAT. ZONE/ FOSSIL CHARACTER				PALEOMAGNETICS	PHYS. PROPERTIES	CHEMISTRY	SECTION	METERS	GRAPHIC LITHOLOGY	DRILLING DISTURB.	SED. STRUCTURES	SAMPLES	LITHOLOGIC DESCRIPTION
	FORAMINIFERS	NANNOFOSSILS	RADIOLARIANS	DIATOMS										
LOWER PLEISTOCENE ?	unzoned early?	PLEISTOCENE	G/A					CC					*	<p>MARLY OOZE</p> <p>Brown (10YR5/4) foraminifer- and nannofossil-rich MARLY OOZE.</p> <p>SMEAR SLIDE SUMMARY (%):</p> <p style="text-align: right;">CC, 0 D</p> <p>TEXTURE:</p> <p>Sand 20 Silt 20 Clay 60</p> <p>COMPOSITION:</p> <p>Clay 20 Foraminifers 32 Nannofossils 40 Radiolarians 2 Sponge spicules 6</p>

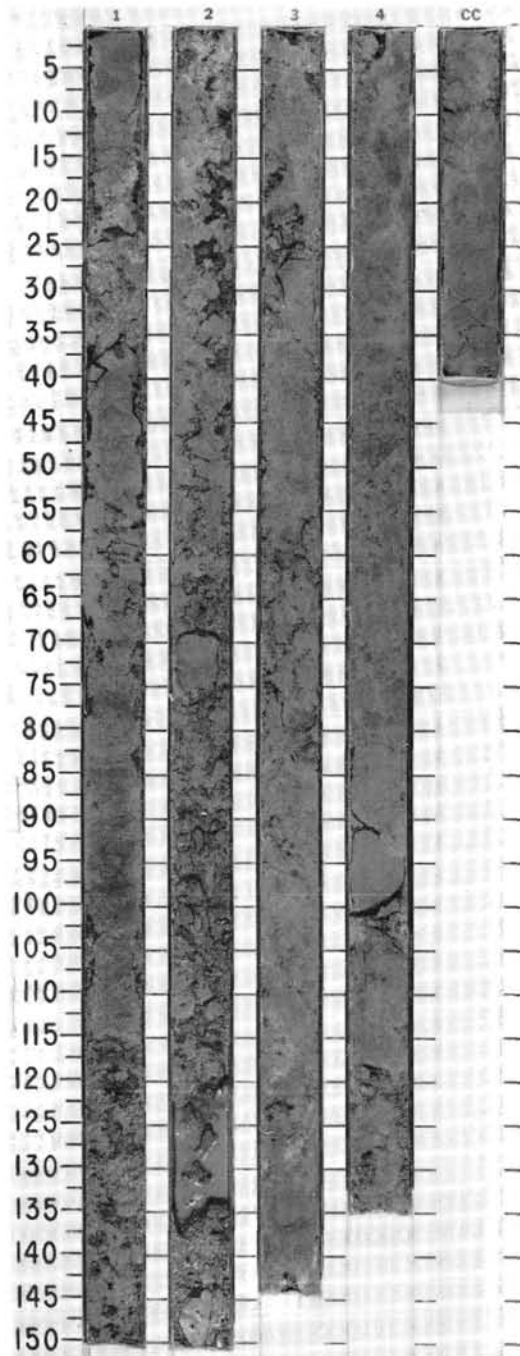


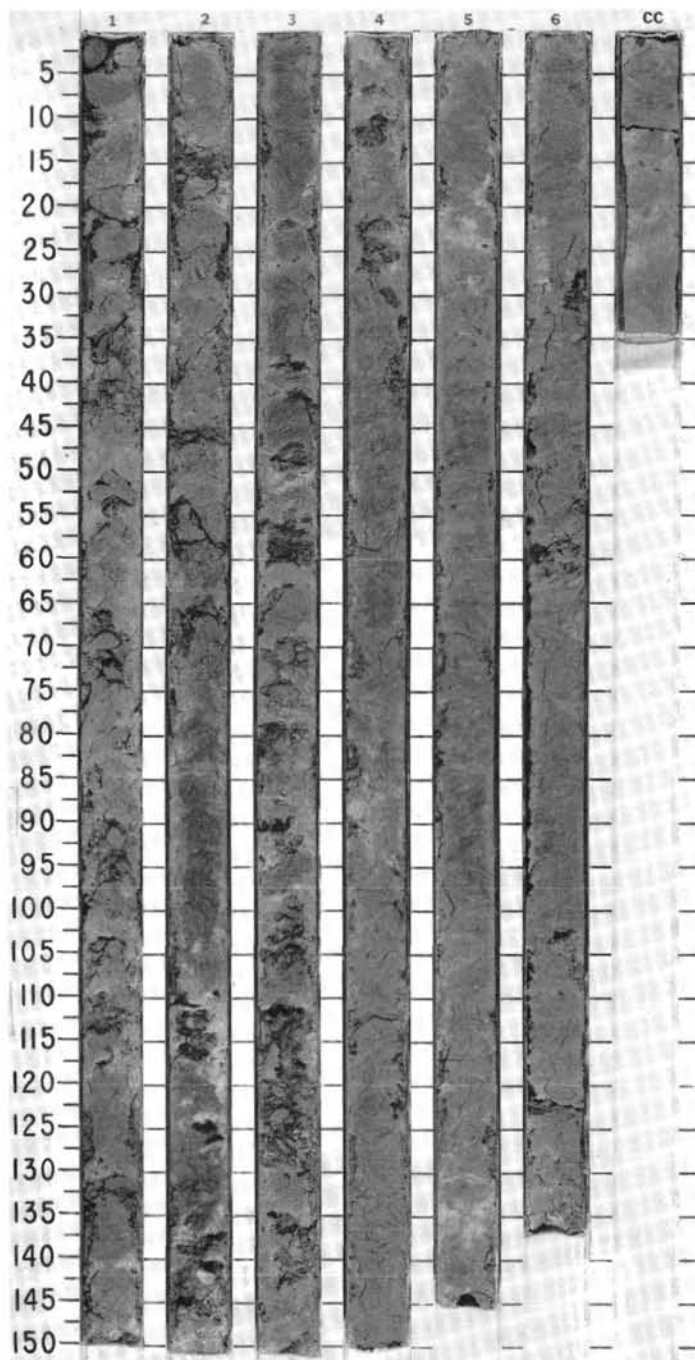
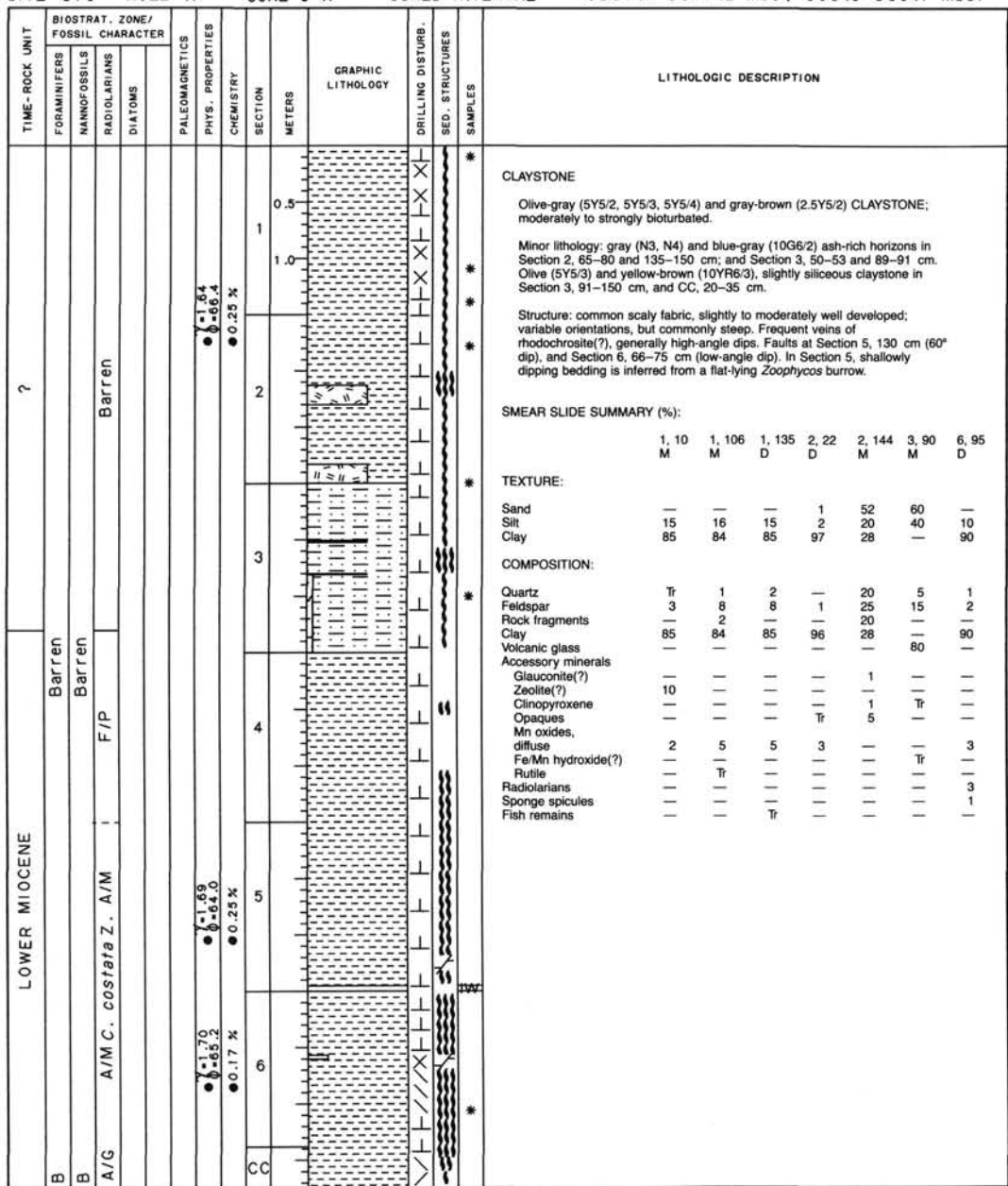
SITE 675 HOLE A CORE 3 X CORED INTERVAL 5339.2-5348.7 mbsl; 331.1-340.6 mbsf

TIME-ROCK UNIT	BIOSTRAT. ZONE/ FOSSIL CHARACTER				PALEOMAGNETICS	PHYS. PROPERTIES	CHEMISTRY	SECTION	METERS	GRAPHIC LITHOLOGY	DRILLING DISTURB.	SED. STRUCTURES	SAMPLES	LITHOLOGIC DESCRIPTION																											
	FORAMINIFERS	NANNOFOSSILS	RADIOLARIANS	DIATOMS																																					
?																																									
B	Barren					● 1.85 ● 8.17 %		1	0.5 1.0					<p>MUDSTONE</p> <p>Olive, olive-green, and green (5Y5/3, 5Y4/2, 10Y5/2, 5GY5/1) MUDSTONE; moderately bioturbated.</p> <p>Minor lithology: 6-mm-thick, black (N3), ashy mudstone layer in Section 2, 100 cm.</p> <p>Structure: pervasive, scaly fabric in Section 1, 0-97 cm; base of scaly interval is a scaly fault zone at 97 cm with scaly foliation immediately above the fault; fault and scaly foliation dip 45°.</p> <p>SMEAR SLIDE SUMMARY (%):</p> <table border="1"> <tr> <td></td> <td>2, 68</td> <td>2, 100</td> </tr> <tr> <td>D</td> <td></td> <td>M</td> </tr> </table> <p>TEXTURE:</p> <table border="1"> <tr> <td>Silt</td> <td>12</td> <td>30</td> </tr> <tr> <td>Clay</td> <td>88</td> <td>70</td> </tr> </table> <p>COMPOSITION:</p> <table border="1"> <tr> <td>Quartz</td> <td>20</td> <td>20</td> </tr> <tr> <td>Clay</td> <td>80</td> <td>63</td> </tr> <tr> <td>Volcanic glass</td> <td>Tr</td> <td>15</td> </tr> <tr> <td>Accessory minerals</td> <td></td> <td></td> </tr> <tr> <td>Pyrite</td> <td>—</td> <td>2</td> </tr> </table>		2, 68	2, 100	D		M	Silt	12	30	Clay	88	70	Quartz	20	20	Clay	80	63	Volcanic glass	Tr	15	Accessory minerals			Pyrite	—	2
	2, 68	2, 100																																							
D		M																																							
Silt	12	30																																							
Clay	88	70																																							
Quartz	20	20																																							
Clay	80	63																																							
Volcanic glass	Tr	15																																							
Accessory minerals																																									
Pyrite	—	2																																							
B	Barren					● 1.73 ● 8.22.1		2																																	
B	Barren					● 1.83 %		3																																	
								CC																																	



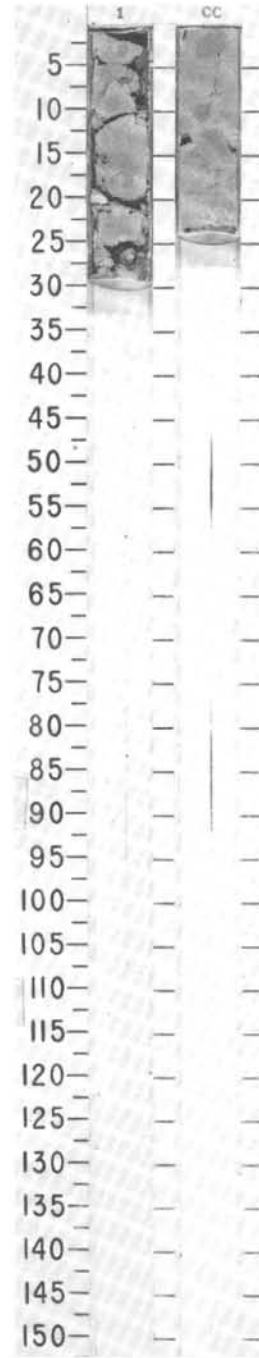
TIME-ROCK UNIT	BIOSTRAT. ZONE/ FOSSIL CHARACTER			PALEOMAGNETICS	PHYS. PROPERTIES	CHEMISTRY	SECTION	METERS	GRAPHIC LITHOLOGY	DRILLING DISTURB.	SED. STRUCTURES	SAMPLES	LITHOLOGIC DESCRIPTION
	FORAMINIFERS	NAUFOSSILS	RADIOLARIANS										
?	Barren	Barren	Barren		$\gamma = 1.66$ $\delta = 65.8$	0.25 %	1			X	X		<p>MUDSTONE</p> <p>Drill breccia composed of clasts of olive (5Y5/2) to olive-green (5GY5/2) MUDSTONE; intensely bioturbated. Many clasts contain patches of dark gray (N4) disseminated ash. Interval in Section 1, 70-115 cm, may be in place.</p> <p>SMEAR SLIDE SUMMARY (%):</p> <p style="padding-left: 40px;">4, 86 D</p> <p>TEXTURE:</p> <p>Silt 25 Clay 75</p> <p>COMPOSITION:</p> <p>Quartz 28 Clay 72 Accessory minerals Pyrite Tr</p>
B	Barren	Barren	Barren		$\gamma = 1.66$ $\delta = 67.5$	0.25 %	2			X	X		
B	Barren	Barren	Barren				3			X	X		
B	Barren	Barren	Barren				4			X	X		
CC										X	X		





SITE 675 HOLE A CORE 7 X CORED INTERVAL 5377.2-5386.7 mbsl; 369.1-378.6 mbsf

TIME-ROCK UNIT	BIOSTRAT. ZONE/ FOSSIL CHARACTER			PALEOMAGNETICS	PHYS. PROPERTIES	CHEMISTRY	SECTION	METERS	GRAPHIC LITHOLOGY	DRILLING DISTURB.	SED. STRUCTURES	SAMPLES	LITHOLOGIC DESCRIPTION						
	FORAMINIFERS	NANNOFOSSILS	RADIOLARIANS																
LOWER MIOCENE	Barren						1					*	MUDSTONE Yellow-brown (10YR6/6) to orange-brown (7.5YR6/6) siliceous MUDSTONE; Section 1 slightly bioturbated. SMEAR SLIDE SUMMARY (%): <table style="margin-left: 40px;"> <tr> <td></td> <td>1, 15</td> <td>CC, 11</td> </tr> <tr> <td></td> <td>D</td> <td>D</td> </tr> </table> TEXTURE: Sand 3 3 Silt 19 13 Clay 78 84 COMPOSITION: Quartz 1 Tr Feldspar 3 1 Clay 78 84 Accessory minerals Opaques Tr Tr Hornblende — Tr Mn oxide 5 — Fe/Mn hydroxides Tr — Radiolarians 10 12 Sponge spicules 3 3		1, 15	CC, 11		D	D
		1, 15	CC, 11																
	D	D																	
Barren						CC						*							
	<i>Stichocorys wolffii</i> Zone A/G																		



TIME-ROCK UNIT	BIOSTRAT. ZONE/ FOSSIL CHARACTER				PALEOMAGNETICS	PHYS. PROPERTIES	CHEMISTRY	SECTION	METERS	GRAPHIC LITHOLOGY	DRILLING DISTURB.	SED. STRUCTURES	SAMPLES	LITHOLOGIC DESCRIPTION																																	
	FORAMINIFERS	NANNOFOSSILS	RADIOLARIANS	DIATOMS																																											
LOWER MIOCENE	B	B	A/P L. elongata Z. A/P	A/M C. tetrapera Z. A/M	1.76 58.4	0.17 %	0.08 %	1	0.5					<p>MUDSTONE and CLAYSTONE</p> <p>Varicolored siliceous MUDSTONE and non- to slightly-siliceous CLAYSTONE; orange-brown (10YR6/4, 10YR5/4) in Section 1, 0-127 cm, grading down to olive (5Y6/3, 5Y5/3), olive-brown (2.5Y5/3, 2.5Y6/3), brown (10YR5/3), and yellow-brown (10YR5/4, 10YR5/6) in Section 1, 127-150 cm, and Section 2 through CC. Overall decrease in siliceous content downcore. Common 1-mm-diameter spherules of zeolite (probable clinoptilolite) throughout.</p> <p>Minor lithology: intervals of black (N1) mudstone in Section 1, 4-8 and 65-68 cm.</p> <p>Structure: poorly developed veins in Section 1, 95-101 cm (70° dip). Fault in Section 2, 113-122 cm (75° dip). Fault zone has moderately well-developed scaly fabric. Low angle, faint, scaly fabric in Section 7.</p> <p>SMEAR SLIDE SUMMARY (%):</p> <table border="1"> <tr> <td></td> <td>1, 100</td> <td>6, 92</td> </tr> <tr> <td></td> <td>D</td> <td>D</td> </tr> </table> <p>TEXTURE:</p> <table border="1"> <tr> <td>Sand</td> <td>10</td> <td>—</td> </tr> <tr> <td>Silt</td> <td>25</td> <td>15</td> </tr> <tr> <td>Clay</td> <td>65</td> <td>85</td> </tr> </table> <p>COMPOSITION:</p> <table border="1"> <tr> <td>Quartz</td> <td>10</td> <td>8</td> </tr> <tr> <td>Feldspar</td> <td>—</td> <td>2</td> </tr> <tr> <td>Clay</td> <td>65</td> <td>82</td> </tr> <tr> <td>Volcanic glass</td> <td>2</td> <td>8</td> </tr> <tr> <td>Radiolarians</td> <td>14</td> <td>—</td> </tr> <tr> <td>Sponge spicules</td> <td>9</td> <td>—</td> </tr> </table>		1, 100	6, 92		D	D	Sand	10	—	Silt	25	15	Clay	65	85	Quartz	10	8	Feldspar	—	2	Clay	65	82	Volcanic glass	2	8	Radiolarians	14	—	Sponge spicules	9	—
		1, 100	6, 92																																												
		D	D																																												
	Sand	10	—																																												
	Silt	25	15																																												
	Clay	65	85																																												
	Quartz	10	8																																												
Feldspar	—	2																																													
Clay	65	82																																													
Volcanic glass	2	8																																													
Radiolarians	14	—																																													
Sponge spicules	9	—																																													
B	B	A/P L. elongata Z. A/P	A/M C. tetrapera Z. A/M	1.76 58.4	0.17 %	0.08 %	2	1.0																																							
A/P	A/P	A/P L. elongata Z. A/P	A/M C. tetrapera Z. A/M	1.76 58.4	0.17 %	0.08 %	3	1.5																																							
?	(unzoned)	A/P	A/M C. tetrapera Z. A/M	1.76 58.4	0.17 %	0.08 %	4	2.0																																							
B	B	A/P L. elongata Z. A/P	A/M C. tetrapera Z. A/M	1.76 58.4	0.17 %	0.08 %	5	2.5																																							
A/P	A/P	A/P L. elongata Z. A/P	A/M C. tetrapera Z. A/M	1.76 58.4	0.17 %	0.08 %	6	3.0																																							
CC	CC	A/P L. elongata Z. A/P	A/M C. tetrapera Z. A/M	1.76 58.4	0.17 %	0.08 %	7	3.5																																							

